

Copyright © 1997 Elsevier Science Ltd

Int. J. Rock Mech. & Min. Sci. Vol. 34, No. 3-4, 1997 ISSN 0148-9062

To cite this paper: *Int. J. Rock Mech. & Min. Sci.* 34:3-4, Paper No. 071B

CHANGES IN ACOUSTIC EVENT PROPERTIES WITH PROGRESSIVE FRACTURE DAMAGE

E. Eberhardt¹; D. Stead²; B. Stimpson³; R.S. Read⁴

¹ Department of Geological Sciences, University of Saskatchewan, Saskatoon, Saskatchewan S7N 5E2, Canada

² Camborne School of Mines, University of Exeter, Redruth, Cornwall TR15 3SE, UK

³ Department of Civil and Geological Engineering, University of Manitoba, Winnipeg, Manitoba R3T 5V6, Canada

⁴ AECL, Whiteshell Laboratories, Pinawa, Manitoba R0E 1L0, Canada

ABSTRACT

Laboratory results from uniaxial compression tests performed on pink Lac du Bonnet granite samples indicate that a number of stages in the progressive failure process of rock can be identified through the combined analysis of strain gauge and acoustic emission (AE) data. Testing focused on identifying the crack initiation (σ_{ci}) and crack damage (σ_{cd}) stress thresholds, two key components in the brittle fracture process. Results from this testing also showed that the properties of the acoustic events are markedly different throughout loading most notably before and after crack initiation. This proved valuable in substantiating observations made using strain gauge data. This paper explores the use of acoustic emissions and the interpretation of the acoustic event properties in identifying the different stages of crack development.

Copyright © 1997 Elsevier Science Ltd

KEYWORDS

Acoustic emissions • crack initiation • event count • ringdown count • peak amplitude • event duration • rise time

INTRODUCTION

The effects of stress induced brittle fracturing on the progressive degradation of intact rock strength is a major concern in assessing the degree of damage that occurs around an underground excavation. Part of this work has concentrated on identifying the different stages of the failure process. Based on axial and lateral deformation measurements recorded during uniaxial and triaxial laboratory tests, these stages have been defined by Brace 1964 and Bieniawski 1967 as being:

- 1) crack closure;
- 2) linear elastic deformation;
- 3) crack initiation and stable crack growth;
- 4) critical energy release (onset of dilatancy) and unstable crack growth;
- 5) failure and post peak behaviour.

Work at Atomic Energy of Canada Limited's (AECL) Underground Research Laboratory (URL) has concentrated on using the crack initiation (σ_{ci}) and crack damage (σ_{cd}) stress thresholds to better quantify rock damage. Martin 1993 has shown that these values are more characteristic of the rock's strength, whereas laboratory derived values of peak strength are dependent on such factors as the loading rate.

The detection of these stress thresholds may prove difficult, especially with respect to crack initiation. Traditionally, crack initiation has been determined through stress-strain analysis as the point where the lateral strain changes from linear to non-linear behaviour (Figure 1). A high degree of error and subjectivity is incorporated into this analysis procedure, especially since lateral strain in rock never truly behaves in a linear fashion (Eberhardt *et al.* 1996).

Acoustic emission techniques have been used with some success in identifying microfracturing in brittle materials. Scholz 1968 found that characteristic AE patterns in rock correlate closely with stress-strain behaviour. However, most of the success in correlating AE activity to microfracturing has involved the latter stages of crack development. This is due to the fact that the majority of AE events occur just prior to failure. The lack of significant AE activity in the initial stages of loading makes it more difficult to distinguish background noise from fracture-related acoustic events. A balance must be struck between setting event threshold limits high enough to filter out the majority of the background noise, yet low enough to pick up the beginning of the microfracturing process.

In addition to recording the number of acoustic events and correlating this number to the measured deformation response in the rock, it is also possible to record certain properties of the AE waveforms. Defined with respect to the event threshold limit (Figure 2), these simple waveform parameters include:

Ringdown Count : The ringdown count is the number of times a signal crosses a preset threshold datum. In general, large events require more cycles to "ring down" to the threshold level and will produce more counts than a smaller event. This provides a measure of the intensity of the acoustic emission event.

Peak Amplitude : The peak amplitude can be related to the intensity of the source in the material producing an acoustic emission. Measurements are generally recorded in log units (decibels, dB) to provide accurate measurement of both large and small signals.

Event Duration : When an acoustic event first crosses the preset threshold, an event detector measures the time that the waveform amplitude remains above the threshold thereby giving the event duration.

Rise Time : The rise time measures the time it takes to reach the peak amplitude of an event. This provides an account of the positive-changing AE signal envelope.

The signal waveform of an acoustic event can be affected by a number of factors including the characteristics of the source, the nature of the medium, the path the waveform travels prior to detection, the sensor characteristics and the recording system. Generally, these waveforms are complex and using them to characterize the source can be difficult. Due to these complexities, AE waveform analysis is best used in a relative sense as a qualitative measurement as opposed to a

quantitative one based on absolute values. However, relatively little work has been done in this area with respect to rock mechanics and the progressive degradation/failure process in rock. A laboratory study was therefore conducted to examine the variations in these waveform properties with respect to the different fracture processes that accompany brittle rock failure.

EXPERIMENTAL PROCEDURE

Uniaxial tests were carried out on cylindrical samples of pink Lac du Bonnet granite taken from the 130 m level of the URL. The pink granite is medium- to coarse-grained with an average grain size between 3 and 4 mm. Samples were prepared from 61 mm diameter cores with length to diameter ratios of approximately 2.25. Considerable care was taken in preparing the sample ends so as to eliminate any excess noise due to the failure of local surface irregularities and cracking associated with undesirable stress concentrations. This entailed the use of a specially constructed frame that allowed for the sample ends to be highly polished. This resulted in measurements of end surface flatness and perpendicularity five times lower than those recommended by ASTM standards (Designation D4543).

Each sample was instrumented with six electric resistance strain gauges (3 axial and 3 lateral at 60° intervals) to record sample deformation and four 175 kHz piezoelectric transducers to record acoustic emissions and related AE properties. Transducers were mounted using wave guides epoxied to the sample surface thereby providing a solid coupling. The monitoring system consists of a bandpass filter with a frequency range of 125 kHz to 1 MHz and a pre-amplifier with 40 dB total gain. The AE data was recorded with an AET 5500 acoustic emission monitoring system using a threshold value of 0.1 V.

Analysis of the laboratory data focused on identifying crack initiation (σ_{ci}) and crack damage (σ_{cd}) stress levels using both strain gauge and AE response. The volume of AE data can sometimes be extremely difficult to handle so an "in-house" program was specifically written to process the data to investigate correlations between the AE event count and several waveform characteristics with stress and time. AE properties including ringdown counts, peak amplitude, event duration and rise time were used in the analysis.

ANALYSIS OF LABORATORY TEST RESULTS

Analysis of the test results show a good correlation between strain gauge data and the AE response. Results show that spikes in the AE count correlate to inflections in the axial, lateral and volumetric stress-strain curves. Figures 3 and 4 show the stress dependent logarithmic acoustic emission event count and volumetric stiffness plots, respectively. The volumetric stiffness plot highlights any rate changes in the volumetric strain and is calculated by differentiating the axial stress vs volumetric strain curve. Volumetric strain itself is calculated from the measured axial and lateral strain response of the sample during uniaxial loading. Eberhardt *et al.* 1996 have shown that the axial, lateral and volumetric stiffness curves can be used to identify crack initiation in addition to several other stages in the brittle fracture process of rock. Results for this analysis, based on 10 uniaxial compression tests, are summarized in Table 1.

Although AE activity occurs continuously throughout the test, the log plot in Figure 3 shows that the beginning of significant AE activity begins at approximately 80 MPa. This coincides with the crack initiation stress (σ_{ci}) of 80 MPa as determined using the volumetric stiffness curve in Figure 4. AE activity prior to this point can be attributed to movement along crack faces during crack closure, as recognized in the lateral strain rate. It is also likely that small cracks may form during low stresses in areas already weakened by stress relief cracking.

Acoustic Event Waveforms

To date, most AE studies have concentrated on using event counts, event rates and source location to analyze sample deformation and failure. A common method of analysis that does focus on the properties of the waveform involves plotting the amplitude distribution (described in Sun *et al.* 1991). However this technique provides little information regarding the gradual changes in amplitude with loading.

Results from this testing show that the properties of the acoustic events are markedly different throughout loading most notably before and after crack initiation. This proves valuable in substantiating observations made using strain gauge data (the results of which are given in Table 1). Figures 5 and 6 contain plots of the event ringdown count and event duration with loading, respectively. Both plots show a marked increase in their respective magnitudes at approximately 80 MPa coinciding with crack initiation. Although acoustic activity occurs prior to this point, the size of the events are relatively small (in terms of event duration, these events are ~70% smaller than those occurring above 80 MPa). This seems to indicate that the acoustic events generated through closure of pre-existing cracks in the samples are much smaller than those generated through the development of new cracks.

The use of ringdown counts and event durations in analyzing sample deformation during uniaxial testing has been mostly as a form of event counting. Nakamura 1997 notes that since the number of threshold crossings per unit time is partly dependent on the resonant characteristics of the transducer, ringdown counting essentially gives a count weighted by the duration of each signal. Ring down count is also directly influenced by the source to detector distance and attenuation (which determines the rate of ring down, thus the duration of the signals). Laboratory derived values of ringdown count are therefore significant only in relative terms. However, as a qualitative measure a correlation can be made between larger ring down counts and event durations with larger acoustic events. Larger events may also indicate the occurrence of different deformation and fracture mechanisms. For example, Sondergeld *et al.* 1984 note that observations of long event durations have been associated with plastic deformation in metals. Figures 5 and 6 indicate that this may also be true for the granite samples, since increases in the respective ringdown count and event duration magnitudes occur at the onset of dilatancy followed by a significantly large increase prior to failure at stress levels where yielding would be expected.

Analysis of the peak event amplitudes (Figure 7) and event rise times (Figure 8) also confirms a number of these observations. Similar to the previous plots, significant increases in the relative values of peak amplitude and event rise time occur at the crack initiation threshold of 80 MPa. These increases are followed by relatively small increases at the onset of dilatancy (~170 MPa) and a large increase prior to failure (~210 MPa) possibly marking the yield point of the sample. It should also be noted that a significant increase in the values for each of the waveform properties occurs between 140 and 150 MPa. This point is reflected in the strain gauge data, as shown in the volumetric stiffness plot (Figure 4), and conceivably points to the beginning of crack coalescence prior to the onset of dilatancy.

These results concur with observations made by Watters, Chuck 1989 who found that the peak amplitude of acoustic events in welded tuff gradually increased throughout loading followed by a significant increase prior to failure. Similar observations were made by Mlakar *et al.* 1993 on samples of potash where increases in event amplitude occurred predominantly at the yield point of the material. In effect, low amplitude AE activity was observed during elastic deformation of the sample followed by high amplitude events after the elastic limit was exceeded. Comparing their results with

scanning electron microscope (SEM) observations, Mlakar *et al.* 1993 concluded that intergranular phenomena present in the early stages in the loading cycle could be associated with low amplitude events. High amplitude events present in the later stages of the loading cycle were associated with intragranular microcracking and transgranular cracking.

Similar errors in measuring the amplitude and rise time occur as those mentioned for the ringdown count and event duration. Waveform attenuation arising from dissipative (i.e. scattering) mechanisms as the wave propagates results in an exponential decrease in wave amplitude with distance. Rise times can be effected by dispersion of the AE wave as well, therefore recorded magnitudes are dependent upon the distance the acoustic emission travels from the source to sensor. In addition, wave forms may travel different paths to reach the sensor. Such multiple paths can lengthen and distort the signal as well as completely distort the rise time (Beattie 1983). Similarly, the value of the peak amplitude may be due to a superposition of several wave forms and have little relationship to the peak value of any of the individual waveforms. However, the results obtained in this study appear to indicate that as a qualitative measure, the peak amplitudes and rise times provide an additional means to corroborate stress-strain data in tracking crack initiation and propagation. When used in this fashion, Beattie 1983 notes that increases in event amplitude may provide significant warning of increasing crack growth rate.

CONCLUSION

A series of uniaxial tests were performed on pink Lac du Bonnet granite samples from the 130 m level of AECL's Underground Research Laboratory (URL) in which both strain gauge and acoustic emission data were collected. A high degree of correlation was seen between the stress-strain data and the AE response in terms of identifying several stages of crack growth in the samples. It was found that this combined use of acoustic emission response and stress-strain analysis provided the most accurate and reliable method of identifying the crack initiation (σ_{ci}) and crack damage (σ_{cd}) stress thresholds, two key components in the brittle fracture process.

AE results suggest that the analysis of acoustic emission data does not need to be restricted to simple AE counts. The measurable characteristics of the event waveform are capable of revealing a number of insights into the progressive failure process of rock. Although a number of mechanisms may be responsible for altering the measured waveforms before they are detected, it was found that when used in a qualitative fashion, observations made using strain gauges can be substantiated.

Examination of the fracture processes in laboratory tested rock will allow for a better understanding of how induced stresses in the near field rock surrounding an excavation or borehole contribute to the strength degradation and failure of the surrounding rock.

Acknowledgments

Parts of the work have been supported by Atomic Energy of Canada, Ltd. and NSERC operating grants. The authors wish to thank Dr. Derek Martin and Zig Szczepanik for their suggestions and contributions into this work. Special thanks are extended to Dr. Emery Lajtai for his insights into the initial stages of the work.

FIGURES

Paper 071B, Figure 1.

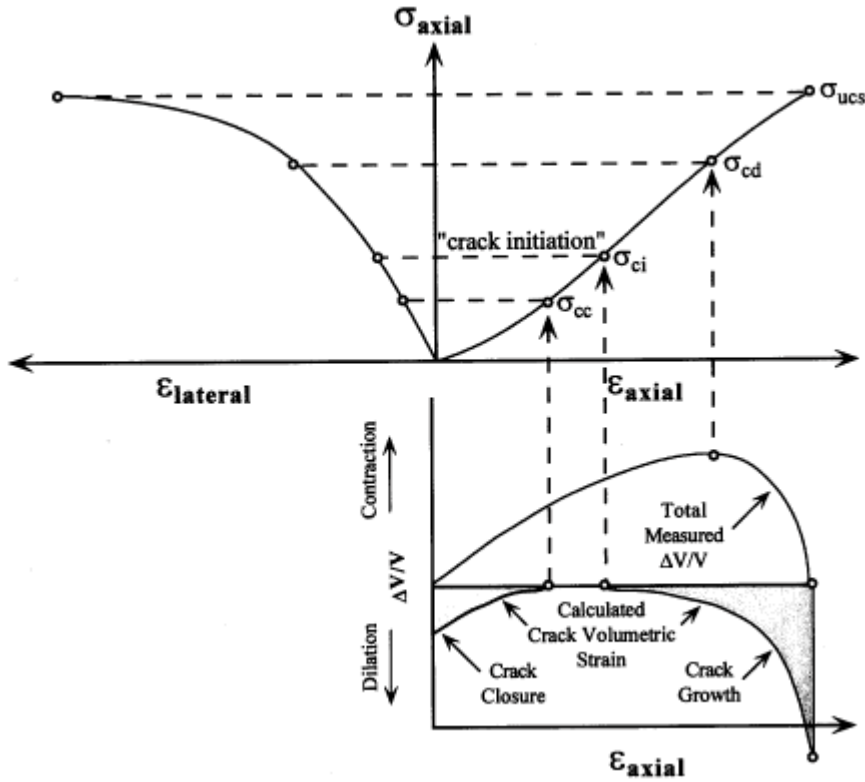


Figure 1. Stress-strain diagram showing the elements of crack development (after Martin 1993). Note that the axial and lateral strains are measured, the volumetric strain and crack volume are calculated.

Paper 071B, Figure 2.

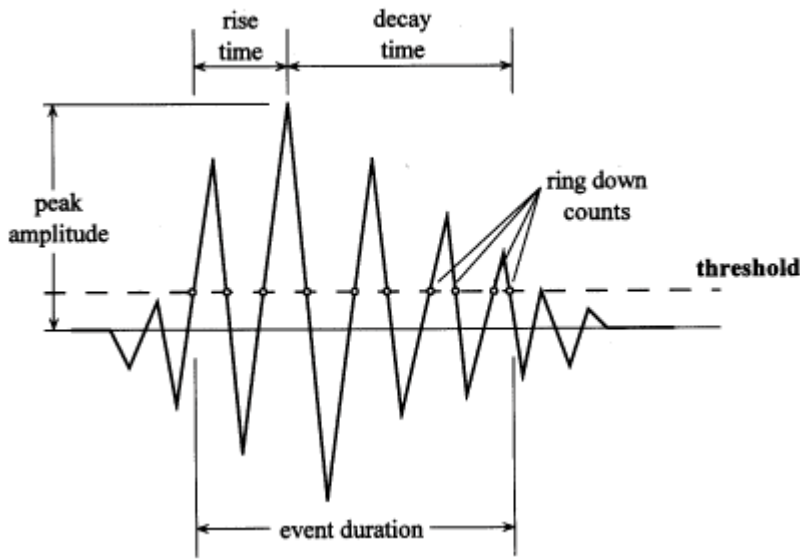


Figure 2. Definition of simple acoustic emission waveform parameters.

Paper 071B, Figure 3.

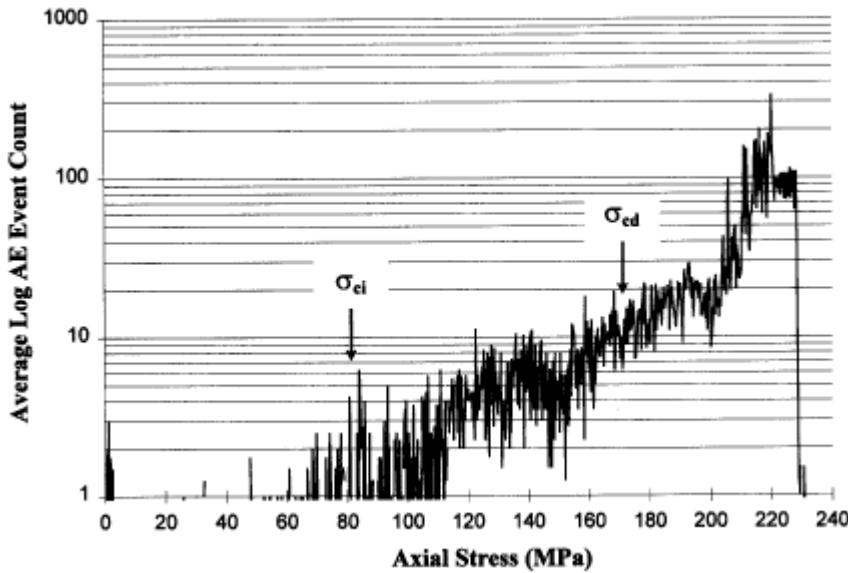


Figure 3. Log acoustic emission response indicating the crack initiation and crack damage stress thresholds for a pink Lac du Bonnet granite.

Paper 071B, Figure 4.

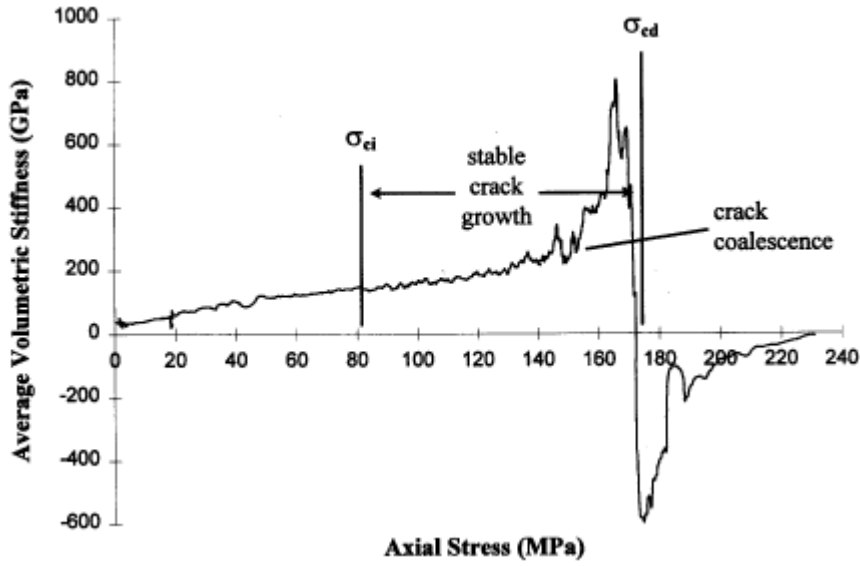


Figure 4. Volumetric stiffness -vs- axial stress for a pink Lac du Bonnet granite. Volumetric stiffness is calculated by differentiating the volumetric strain -vs- axial stress curve.

Paper 071B, Figure 5.

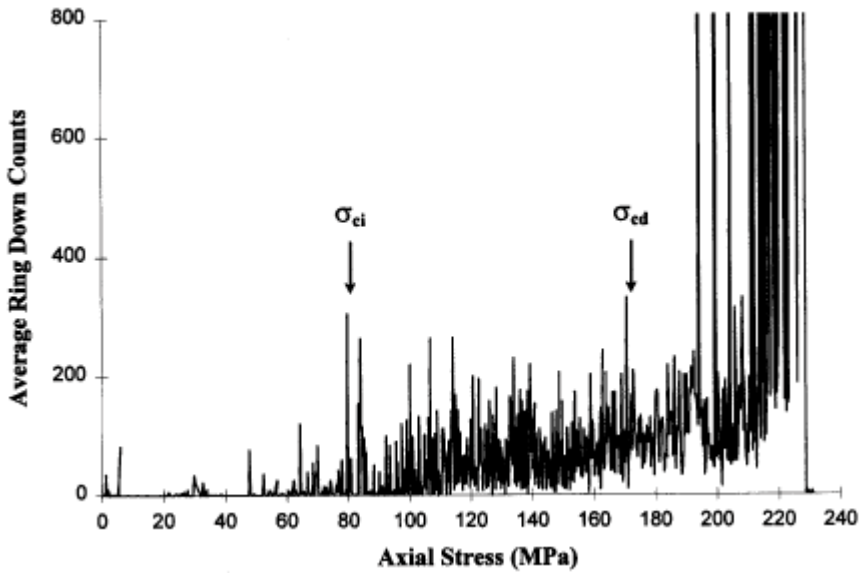


Figure 5. AE event ringdown counts -vs- axial stress for a pink Lac du Bonnet granite.

Paper 071B, Figure 6.

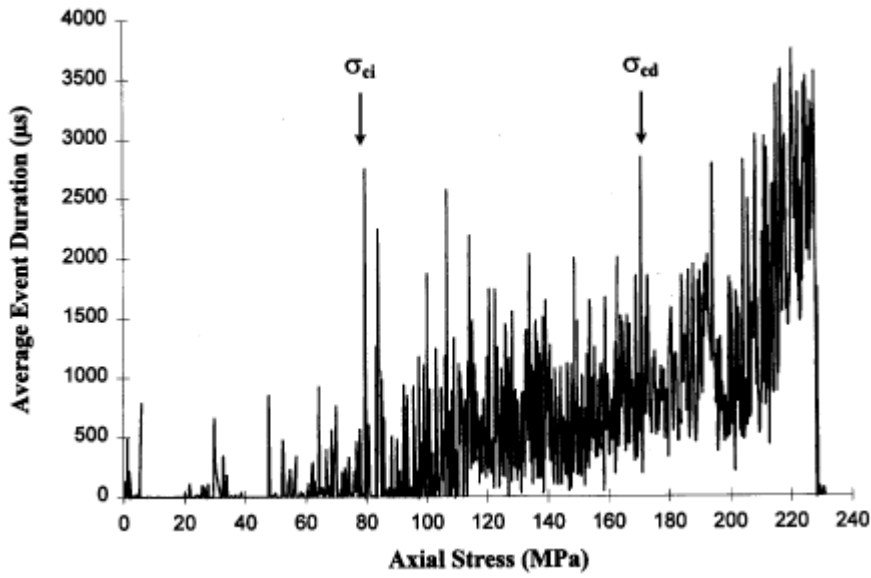


Figure 6. AE event durations -vs- axial stress for a pink Lac du Bonnet granite.

Paper 071B, Figure 7.

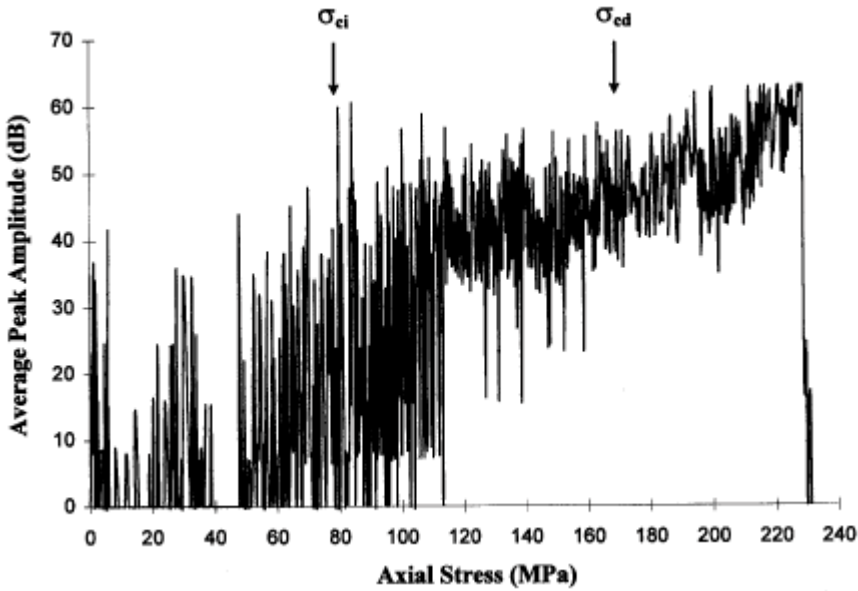


Figure 7. AE event peak amplitude -vs- axial stress for a pink Lac du Bonnet granite.

Paper 071B, Figure 8.

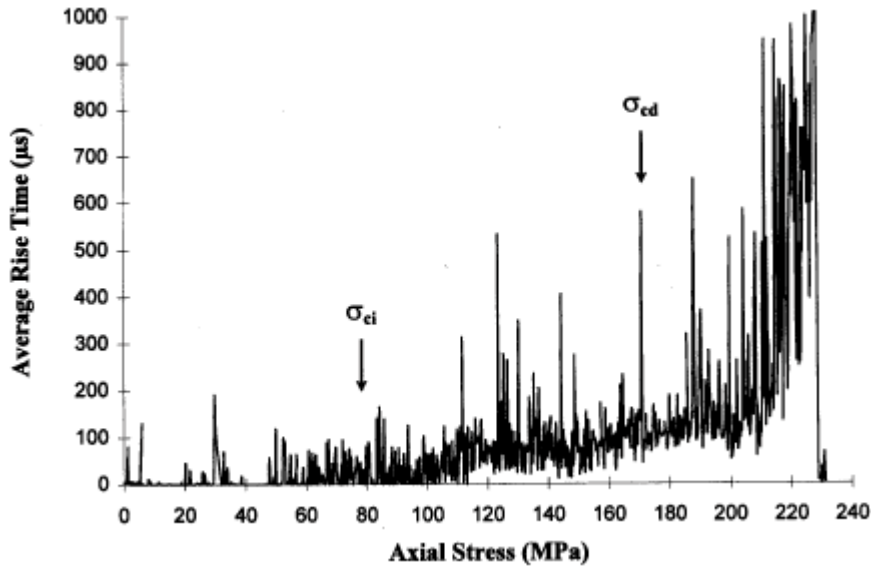


Figure 8. AE event rise times -vs- axial stress for a pink Lac du Bonnet granite.

TABLES

Paper 071B, TABLE 1.

TABLE 1

**AVERAGE STRENGTH PARAMETERS FOR URL PINK GRANITE
(STANDARD DEVIATION IS IN PARENTHESES)**

Property	130m Level Pink Granite
Crack Closure, σ_{cc}	46.4 (\pm 3.2) MPa
Crack Initiation, σ_{ci}	83.2 (\pm 4.1) MPa
Crack Damage, σ_{cd}	162.2 (\pm 11.8) MPa
Peak Strength, σ_{UCS}	213.1 (\pm 12.0) MPa

References

References

- Beattie A.G. 1983. Acoustic emission, principles and instrumentation. *Journal of Acoustic Emission*, **2:1/2**, 95–128.
- Brace W.F. 1964. Brittle fracture of rocks. In *State of Stress in the Earth's Crust: Proceedings of the International Conference, Santa Monica*, W.R. Judd, Ed., American Elsevier, New York, pp. 110–178.
- Bieniawski Z.T. 1967. Mechanism of brittle rock fracture: Part 1 - Theory of the fracture process. *International Journal of Rock Mechanics and Mining Sciences & Geomechanical Abstracts*, **4:4**, 395–406.
- Eberhardt E., Stead D., Szczepanik Z. 1996. *Crack Initiation and Propagation in Granite and Granodiorite from the 130m and 420m Levels of the URL*. Atomic Energy of Canada, Ltd. Report #122567.
- Martin C.D. 1993. *The Strength of Massive Lac du Bonnet Granite Around Underground Openings*, PhD Thesis, Department of Civil and Geological Engineering, University of Manitoba, Canada.
- Mlakar V., Hassani F.P., Momayez M. 1993. Crack development and acoustic emission in potash rock. *International Journal of Rock Mechanics and Mining Sciences & Geomechanical Abstracts*, **30:3**, 305–319.
- Nakamura Y. 1977. Detection and analysis of acoustic emission signals. In *Proceedings of the First Conference on Acoustic Emission/Microseismic Activity in Geologic Structures and Materials, University Park*, H.R. Hardy Jr. and F.W. Leighton, Eds., Trans Tech Publications, Germany, pp. 445–457.
- Scholz C.H. 1968. Microfracturing and the inelastic deformation of rock in compression. *Journal of Geophysical Research*, **73:4**, 1417–1432.
- Sondergeld C.H., Granryd L.A., Estey L. H. 1984. Acoustic emissions during compression testing of rock. In *Proceedings of the Third Conference on Acoustic Emission/Microseismic Activity in Geologic Structures and Materials, University Park*, H.R. Hardy Jr. and F.W. Leighton, Eds., Trans Tech Publications, Germany, pp. 131–145.
- Sun X., Hardy Jr. H.R., Rao M.V.M.S. 1991. Acoustic emission monitoring and analysis procedures utilized during deformation studies on geologic materials. In *Acoustic Emission: Current Practice and Future Directions, ASTM STP 1077*, W. Sachse, J. Roget and K. Yamaguchi, Eds., American Society for Testing and Materials, Philadelphia, pp. 365–380.
- Watters R.J., Chuck D.M. 1989. Acoustic emission signatures of Yucca Mountain tuffs, Nevada. In *Rock Mechanics as a Guide for Efficient Utilization of Natural Resources: Proceedings of the 30th U.S. Symposium, Morgantown*, A.W. Khair, Ed., A.A. Balkema, Rotterdam, pp. 245–252.